Michael U. Kumke, Sascha Eidner

Fluorescence and energy transfer processes of humic substances and related model compounds in terbium complexes

first published in:
Humic Substances: Molecular Details and Applications in Land And Water Conservation / Elham A. Ghabbour, Geoffrey Davies. - 2005, p. 131 - 152
ISBN: 9781591690313

Postprint published at the institutional repository of Potsdam University:
In: Postprints der Universität Potsdam :
Mathematisch-Naturwissenschaftliche Reihe ; 10
http://opus.kobv.de/ubp/volltexte/2007/1225/
http://nbn-resolving.de/urn:nbn:de:kobv:517-opus-12255

Postprints der Universität Potsdam
Mathematisch-Naturwissenschaftliche Reihe ; 10

FLUORESCENCE AND ENERGY TRANSFER PROCESSES OF HUMIC SUBSTANCES AND RELATED MODEL COMPOUNDS IN TERBIUM COMPLEXES

Michael U. Kumke[1] and Sascha Eidner[1]

[1]Institute of Chemistry, University of Potsdam, Karl-Liebknecht-Str. 24-25, 14476 Potsdam-Golm, Germany

Abstract

The fluorescence properties and the fluorescence quenching by Tb^{3+} of substituted benzoic acid were investigated in solution at different pH. The substituted benzoic acids were used as simple model compounds for chromophores present in humic substances (HS). It is shown that the fluorescence properties of the model compounds resemble fluorescence of HS quite well. A major factor determining the fluorescence of model compounds are proton transfer reactions in the electronically excited state. It is intriguing that the fluorescence of the model compounds was almost not quenched by Tb^{3+} while the HS fluorescence was decreased very effectively. From our results we concluded that proton transfer reactions as well as conformational reorientation processes play an important role in the fluorescence of HS.

The luminescence of bound Tb^{3+} was sensitized by an energy transfer step upon excitation of the model compounds and of HS, respectively. For HS the observed sensitization was dependent on its origin indicating differences 1) in the connection between chromophores and binding sites and 2) in the energy levels of the chromophore triplet states. Hence, the observed sensitization of the Tb^{3+} luminescence could be useful to characterize structural differences of HS in solution.

Interlanthanide energy transfer between Tb^{3+} and Nd^{3+} was used to determine the average distance *R* between both ions using the well-known formalism of luminescence resonance energy transfer. *R* was dependent on the origin of the HS reflecting the difference in structure. The value of R_{min} seemed to be a unique feature of the HS. It was further found that upon variation of the pH *R* also changed. This demonstrates that the measurement of interlanthanide energy transfer can be used as a direct method to monitor conformational changes in HS.

1. INTRODUCTION

In the past the quenching of the intrinsic humic substances (HS) fluorescence upon complexation with metal ion was employed in order to calculate the binding constant β.[1–4] Synchronous fluorescence, excitation-emission matrices, and lanthanide ion probe spectroscopy have been applied as experimental techniques in order to elucidate the binding of metal ions by HS.[5-13] It has been pointed out that the main draw backs are the unknown stoichiometry of the metal-HS complex and the unknown source of the intrinsic HS fluorescence both are directly related to the lack of information on the HS structure.[14-17]

However, the application of fluorescence techniques for the determination of β is very attractive, because no separation step is involved, they are applicable at environmental relevant concentrations, and the system investigated experiences only a minor disturbance by the excitation light. Major limitations in the application of fluorescence techniques for the determination of β arise from the lack of understanding of the complex intra- and intermolecular processes that are involved in the HS fluorescence. In order to shed more light into these processes we approached the problem by using "simple" substituted benzoic acids as model compounds for HS in order to elucidate the elemental fluorescence processes of HS. The complexation of lanthanide ions by humic substances (HS) and model compounds was investigated using steady-state and time-resolved luminescence spectroscopic techniques. In the luminescence measurements the fluorescence of the HS and of the substituted benzoic acids as model compounds for HS chromophores was recorded together with the intrinsic luminescence of Tb^{3+}. The selection of the model compounds was driven by 1) more and more experimental evidence that the size of HS is rather small compared to the suggestions made earlier[18], 2) the presence of model-compound-related structures in precursor materials, like lignins, and 3) analytical data obtained from degradation experiments like enzymatic

hydrolysis.[19] Based on these facts we chose different substituted benzoic acids, like salicylic acid or 3,5-dihydroxy benzoic acid as "simple" model compounds.

In the first part of the paper we compared the fluorescence properties with those of HS. Special emphasis was given to the time-resolved fluorescence of model compounds and of HS and how the fluorescence decay kinetics were changed upon Tb^{3+} complexation.

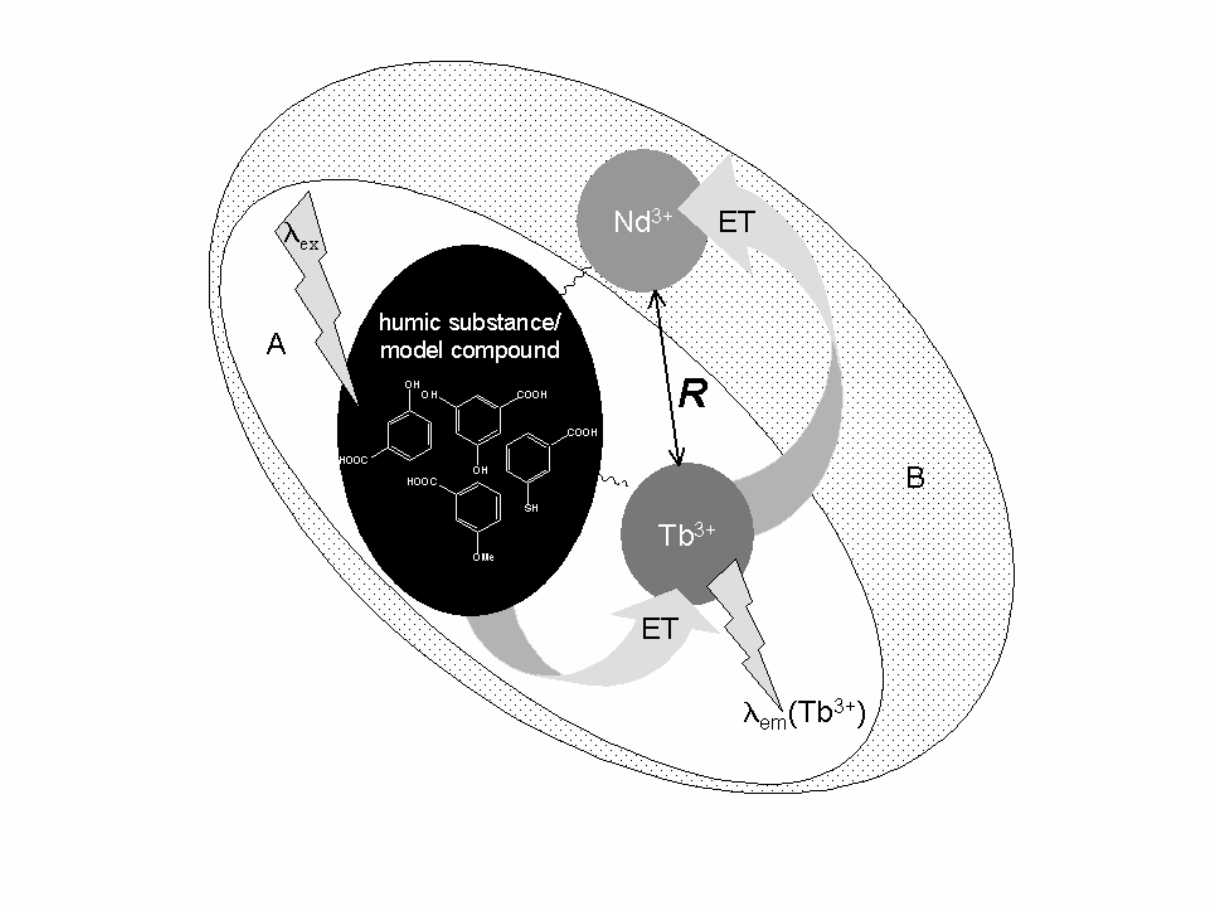

Scheme 1 Investigated energy transfer processes for A) the interaction between HS (or model compound) and Tb^{3+} and B) the interlanthanide energy transfer between Tb^{3+} and Nd^{3+} for the determination of *R*.

In the second part of the paper we investigated the energy transfer from HS and from model compounds to complexed Tb^{3+} and measured the quenching of the intrinsic

fluorescence of the ligands as well as the luminescence enhancement of complexed Tb^{3+} (see Scheme 1). Furthermore, the interlanthanide energy transfer between Tb^{3+} and Nd^{3+} both bound to HS was employed in order to calculate the (average) distance *R* between Tb^{3+} and Nd^{3+} in HS (see Scheme 1). The distance calculations were based on the well-established concept of resonance energy transfer introduced by Förster.[20-22]

2. MATERIALS AND METHODS

2.1 Materials

The substituted benzoic acids (benzoic acid, 3-methoxy benzoic acid, 3,5-dihydroxy benzoic acid, salicylic acid, mercapto salicylic acid, and gallic acid) were purchased from Aldrich and used without further purification. In the experiments the concentration of the substituted aromatic benzoic acid was set to 10^{-4} M.

Several HS samples were employed in the study with a focus on Suwannee River fulvic acid (SRFA). Commercially-available humic substances were purchased from Aldrich and from the International Humic Substances Society (Peat HA, Leonardite HA, Soil HA, Suwannee River HA (SRHA)). HS was also isolated from soil seepage water (BS1 HA) and from a brown water lake (HO13 HA).[23] The HS samples were investigated at a constant pH of 5, and at constant ionic strength (I = 0.02 M). The SRFA sample was also investigated at pH 3, 4, 5, and 6 at a constant ionic strength (I = 0.02 M). The pH of solutions was adjusted using HCl and NaOH. The lanthanide ions were added using 0.001 M stock solutions of nitrates of Tb^{3+}, Nd^{3+}, and La^{3+}. All solutions were stored in the dark until used. In the investigation of the inter-lanthanide energy transfer typically 3 ml of a HS solution (10 mg/L, pH and I = const) and 30 μl of Tb^{3+} (same pH and I) were mixed and equilibrated for 5 min yielding a

concentration of Tb^{3+} of ~10^{-5} M. The Tb^{3+} luminescence was recorded and subsequently in steps of 5 µl a solution containing a second lanthanide ion (Nd^{3+} or La^{3+} with $c_{Ln} = 10^{-3}$ M) was added, equilibrated and then measured up to final overall metal concentrations of ~$5*10^{-5}$ M.

2.2 Methods

Steady-state fluorescence data were acquired with a FluoroMax III spectrometer (Jobin-Yvon, Grasbrunn, Germany) equipped with a R928P photomultiplier tube. The slits were set to a 2 nm spectral band pass in excitation and 4 nm spectral band pass in the emission. In the steady-state fluorescence experiments with HS, an excitation wavelength of λ_{ex} = 325 nm was applied and the HS fluorescence was measured in the wavelength range between 375 nm < λ_{em} < 640 nm. The spectra were evaluated at a Tb^{3+}-luminescence peak (λ_{em} = 544 nm). In case of the substituted benzoic acids the excitation wavelength was chosen according to the absorption maximum of the compound (located at the highest wavelength range). Depending on the particular compound an excitation wavelength λ_{ex} between 300 nm < λ_{ex} < 335 nm was employed.

Time-resolved fluorescence experiments were performed with a FL920 lifetime spectrometer (Edinburgh Instruments, UK). The instrument was equipped with a R955 photomultiplier operated in the single photon counting mode. A N_2 laser (LTB, Berlin, Germany) with λ_{ex} = 337.1 nm was used as excitation source with a repetition rate of 20 Hz. The terbium luminescence was detected at λ_{em} = 544 nm ($^5D_4$ – $^7F_5$ transition). The data were analyzed by standard least square algorithms of a commercial software package (Edinburgh Instruments, UK). All fluorescence measurements were carried out at 293 K.

Time-resolved emission spectra (TRES) were measured using a streak camera system. For the excitation of the samples a mode-locked Ti:sapphire laser (Tsunami, Spectra Physics, Germany) was used. If not otherwise noted, the samples were excited after third harmonic generation at λ_{ex} = 280 nm. The FWHM of the laser pulse was 100 fs. The fluorescence of the samples was detected by a streak camera (C5680, Hamamatsu, Germany) equipped with an imaging spectrograph (250is, Chromex). The streak camera was operated in the sync mode at 80.2 MHz. The time-resolved measurements were performed using two time windows of 3495 ps and 1998 ps, respectively. The TRES were recorded in the single photon counting mode. For each TRES 10000 images (304 ms integration time each) were accumulated. The fluorescence decay time were calculated from the TRES by evaluating slices of $\Delta\lambda_{em}$ = 10 nm using a lifetime fitting module (TA-Fit, Hamamatsu).

3. RESULTS

3.1 Intrinsic fluorescence of "simple" organic ligands

Fluorescence techniques are powerful tools for the investigation of intermolecular interactions like metal complexation. However, for HS the connection between structure and also possible contribution from intramolecular processes is still not fully understood.[24,25] In order to elucidate the contributions of various possible intramolecular processes (*vide infra*), we chose different "simple" substituted benzoic acids as model compounds for HS and investigated their fluorescence characteristics.

In comparison to the HS fluorescence, the fluorescence of the model compounds showed similar characteristics and dependencies on solution parameters, e.g., the spectral

range of emission, broad and featureless emission spectra with a strong dependence on the pH of the solution (see Figure 1).[26-38]

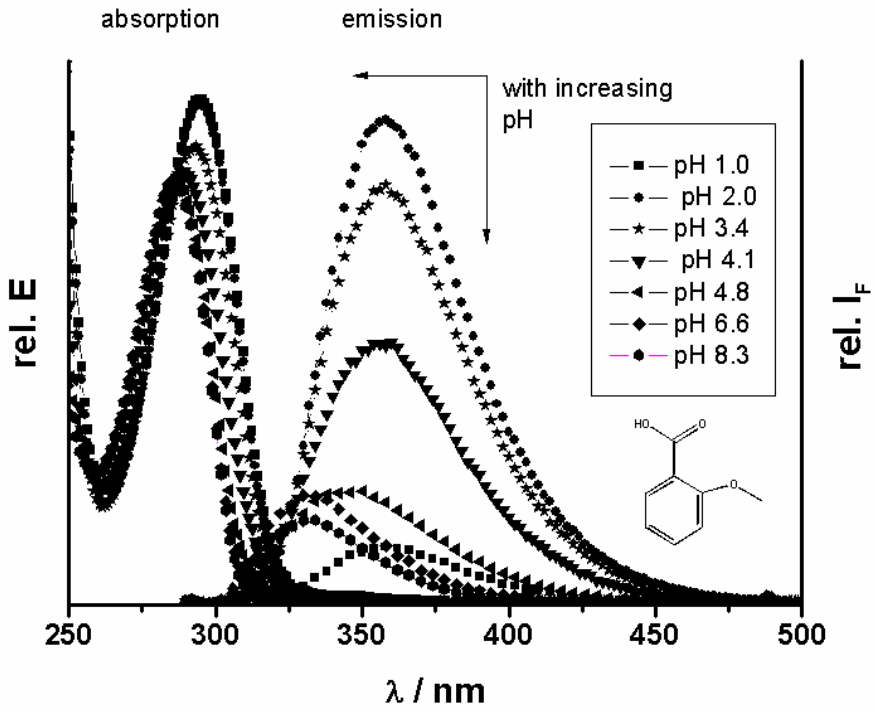

Figure 1 Absorption and fluorescence spectra of 3-methoxy benzoic acid (c = 10^{-4} M) are shown for different pH. In the fluorescence measurements the excitation wavelength λ_{ex} was set to 285 nm.

In Figure 1, as an example the pH dependence of the absorption and the fluorescence of 3-methoxy benzoic acid is shown. The fluorescence efficiency as well as the location of the emission maximum changed with varying pH. It was shifted towards shorter wavelengths and the fluorescence intensity decreased except for pH 1, here, the smallest fluorescence intensity was observed. The blue shift was also observed for the longest absorption band.

The time-resolved emission spectra (TRES) of the model compounds were also measured. As an example, in Figure 2 the TRES of 3,5-dihydroxy benzoic acid is shown at pH 2 (top) and at pH 5 (bottom). Presented are the fluorescence spectra (x-axis) as a function of time (y-axis) after excitation on a picosecond time scale. The corresponding fluorescence intensities are represented by a grey scale.

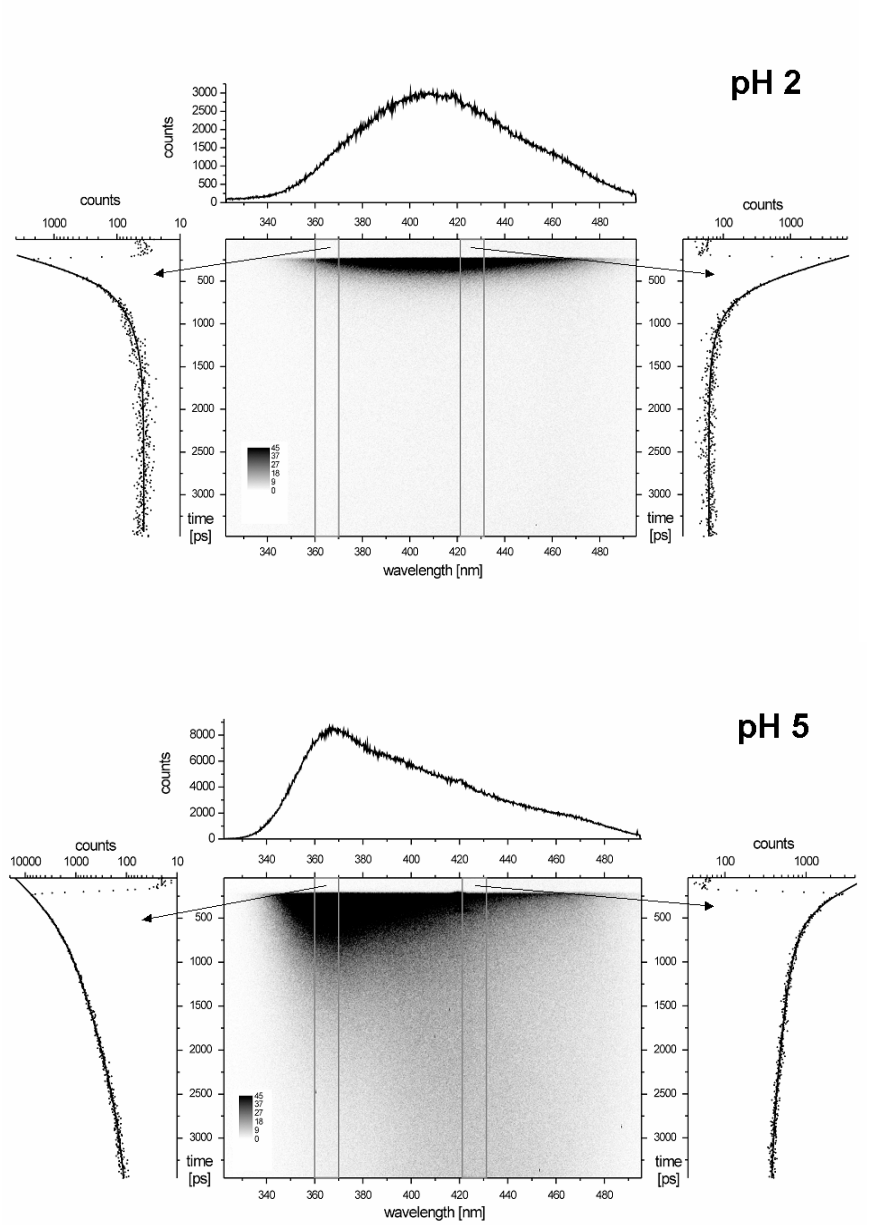

Figure 2 The TRES of 3,5-dihydroxy benzoic acid (c = 10^{-4} M) at pH 2 (top) and pH 5 (bottom) were obtained with an excitation wavelength λ_{ex} = 280 nm, the FWHM of the excitation pulse was 100 fs. On top of the TRES the steady state fluorescence spectrum calculated from the TRES spectrum is shown. On the left and right hand side fluorescence decay curves for the wavelength range 360 nm < λ_{em} < 370 nm and 422 nm < λ_{em} < 432 nm are presented.

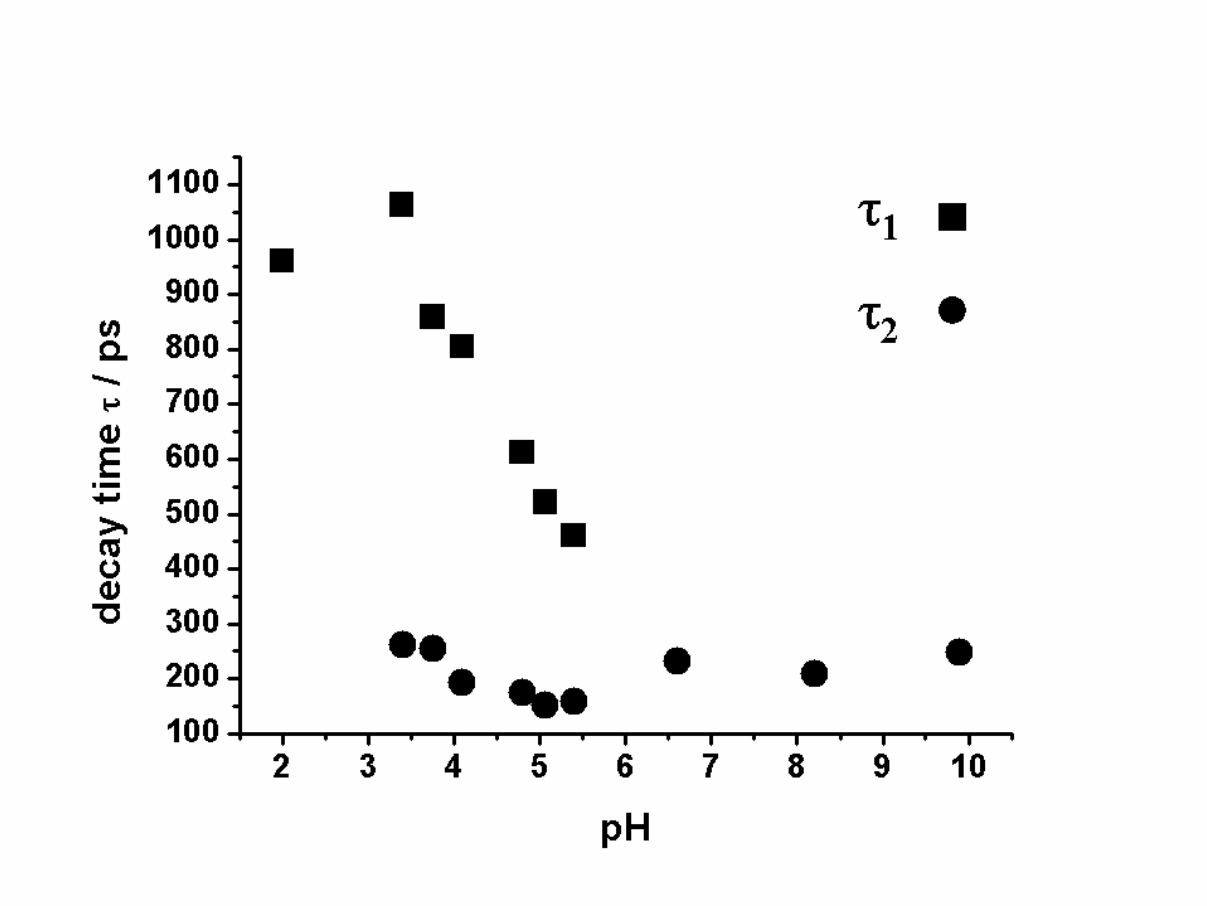

Figure 3 Fluorescence decay times of 3-methoxy benzoic acid (c = 10^{-4} M) at different pH. The fluorescence decay curves were extracted from the TRES (λ_{ex} = 280 nm, 365 nm < λ_{em} < 385 nm).

In Figure 2 on top of each TRES the steady-state fluorescence spectrum is shown. By changing the pH the TRES were heavily influenced. At very low (pH < 2) and very high (pH > 10) pH the observed fluorescence decay of the model compounds (e.g., 3,5-dihydroxy benzoic acid, 3-methoxy benzoic acid) followed basically a mono-exponential decay law indicating that only one species was involved in the fluorescence process (see top of Figure 2 for examples of fluorescence decay curves). This is further supported by the shape of the fluorescence spectrum during the excited state lifetime. At very low and at high pH no shift of the emission maximum during the excited state lifetime was observed in the TRES. However, in the pH range between 2 < pH < 10 a complex fluorescence decay was found as well as a

shift of the emission maximum. In Figure 3 as an example the results of the analysis of the fluorescence decays of 3-methoxy benzoic acid at different pH are shown. The fluorescence decays were analysed by a mono- or bi-exponential decay law depending on the pH of the sample. The fitted decay times are plotted as a function of pH. It can be seen that in the medium pH range the fluorescence decay of 3-methoxy benzoic acid follows a complex, bi-exponential decay law.

Moreover, for the medium pH range the spectral shape and also the location of the fluorescence maximum observed in TRES of the investigated model compounds changed during the excited state lifetime. A comparison of the fluorescence decay at the blue edge and the red edge of the TRES of 3,5-dihydroxy benzoic acid (Figure 2, bottom) stresses the spectral shift of the fluorescence maximum during the fluorescence lifetime of the model compounds. While on the blue edge (left decay in Figure 2, bottom) the fluorescence decay is relative short, it becomes much longer at higher wavelengths (right decay in Figure 2, bottom) indicating a shift in the emission maximum with time.

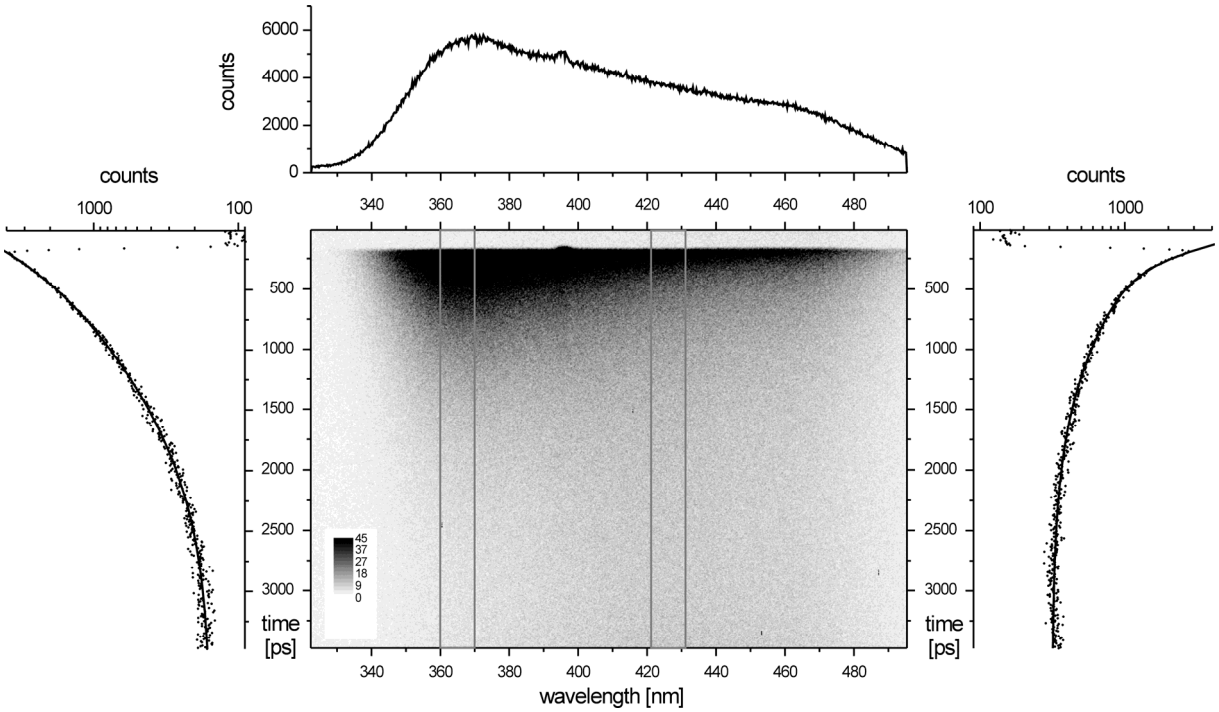

Figure 4 TRES of 3,5-dihydroxy benzoic acid (c = 10^{-4} M) in the presence of Tb^{3+} at pH 5 at a molar ratio of 1:1 (λ_{ex} = 265 nm). Also shown are the fluorescence decay curves (on the left and right for the wavelength ranges 360 nm < λ_{em} < 370 nm and 422 nm < λ_{em} < 432 nm, respectively) and the steady-state fluorescence spectrum (top, the little peak at ~398 nm is a minor contribution from scatter light of the second harmonics of the Ti:Sapphire laser). For corresponding the fluorescence decay time see Table 1.

Table 1 Comparison of the fluorescence decay times of 3,5-dihydroxy benzoic acid and 3-methoxy benzoic acid (c = 10^{-4} M) in the absence and presence of Tb^{3+} (c_{Tb} = 10^{-4} M) at pH 5.

			addition of Tb^{3+}	
	τ_1 / ps	τ_2 / ps	τ_1 / ps	τ_2 / ps
3,5-dihydroxy benzoic acid				
350-360nm	202	**736**	183	**607**
422-432nm	162	**1297**	98	**592**
3-methoxy benzoic acid				
345-365nm	143	1022	152	1036
390-420nm	208	4122	226	4022

In Figure 4 the TRES of 3,5-dihydroxy benzoic acid at pH 5 in presence of Tb^{3+} ions is shown and in Table 1 the results of the analysis of the fluorescence decays at 360 nm < λ_{em} < 370 nm and at 422 nm < λ_{em} < 432 nm are compared with corresponding lifetime data in the absence of Tb^{3+} (see also Figure 2, bottom). It is striking that due to the complexation of the lanthanide ions the temporal and spectral evolution of the TRES is altered. While in the absence of Tb^{3+} a shift in the emission maximum and a complex, emission wavelength-dependent fluorescence decay was found at pH 5, those effects were almost eliminated upon addition of Tb^{3+}. This can also be seen from the calculated fluorescence decay times for the different spectral ranges. In the absence of Tb^{3+} τ_2 differs almost by a factor of two while in the presence of Tb^{3+} equal values for τ_2 were found (see Table 1). It is interesting to note that in case of 3-methoxy benzoic acid no influence of Tb^{3+} on the fluorescence decay was observed (see also Table 1). This might stress the importance of hydroxyl groups in the interaction with metal ions and on the subsequent fluorescence processes.

3.2 Energy-transfer from ligands to lanthanide ions

The effect of Tb^{3+} addition on the intrinsic fluorescence of model compounds and HS was investigated.

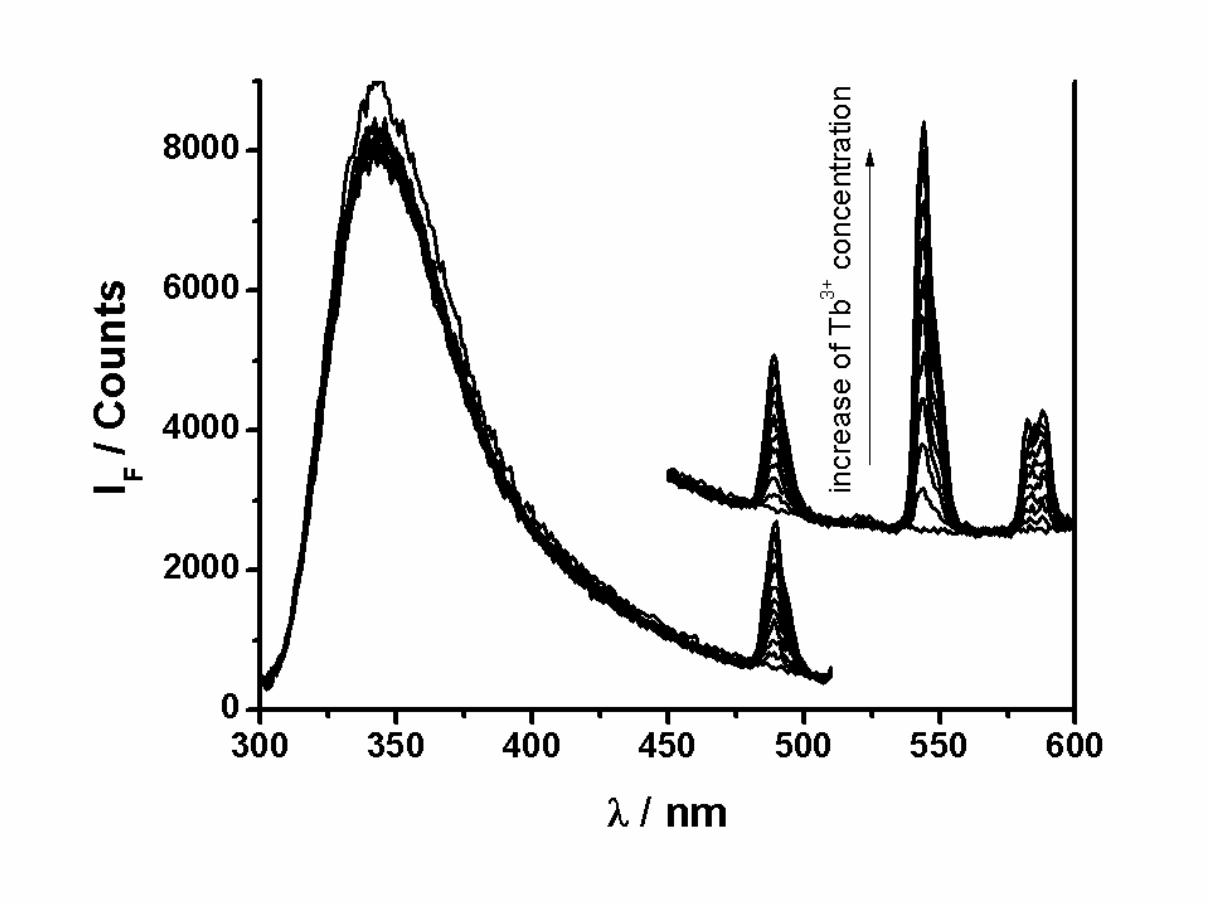

Figure 5 Steady-state fluorescence spectra of gallic acid (c = 10^{-4} M) at pH 4 with increasing Tb^{3+} concentration. (c_{Tb} *10^{-4} = 0.4, 0.8, 1.2, 1.6, 2, 2.3, 2.7, 3.1, 3.5, 3.8). Shown is also the luminescence of Tb^{3+}. The fluorescence was excited at λ_{ex} = 295 nm).

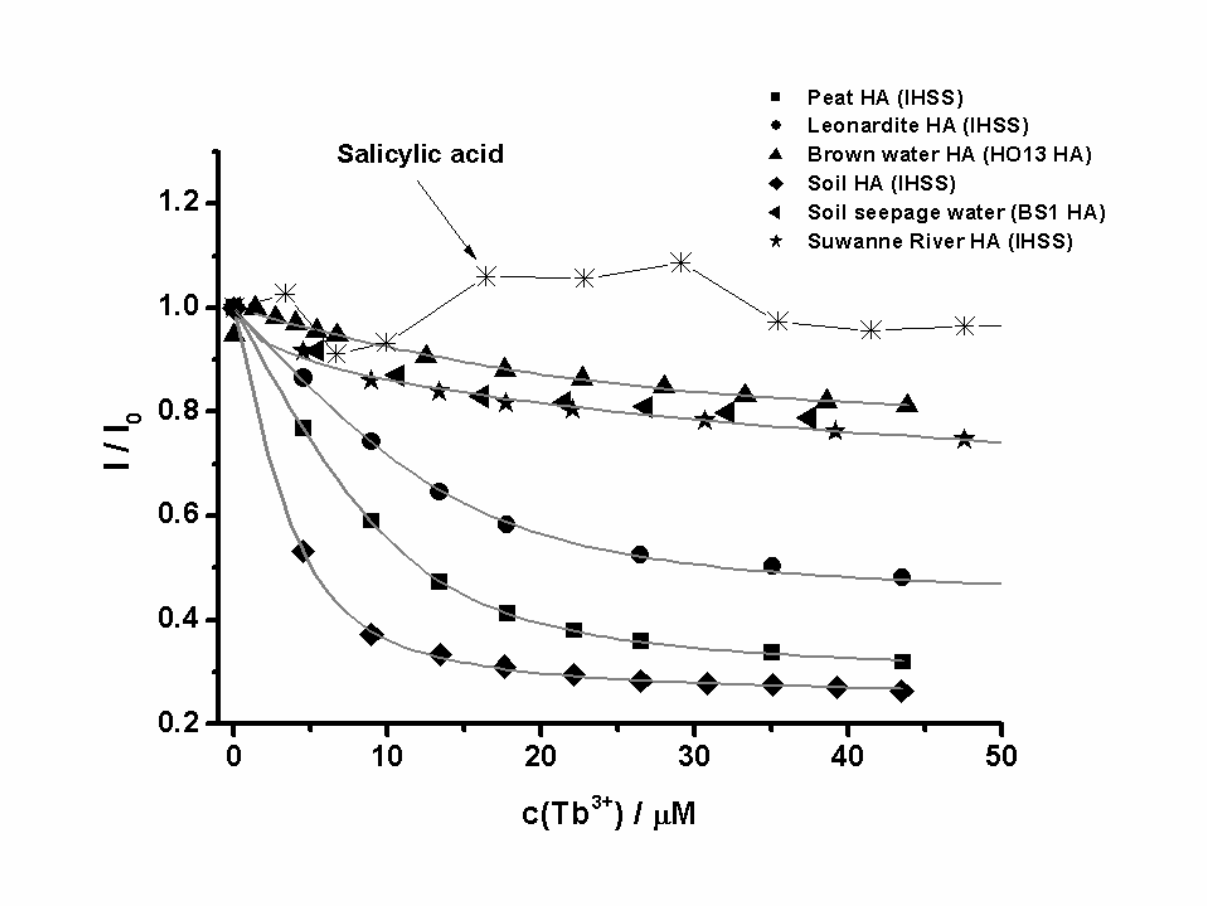

Figure 6 Quenching of the intrinsic fluorescence of HS of different origin upon addition of Tb^{3+}. Shown is further the effect of Tb^{3+} on the fluorescence of salicylic acid. In case of HS the concentration of all samples was 10 mg/L and the pH was adjusted to 5 (λ_{ex} = 325 nm, 425 nm < λ_{em} < 475 nm).

In Figure 5 fluorescence spectra of gallic acid (c = 10^{-4} M) with increasing concentration of Tb^{3+} are shown. Upon addition of Tb^{3+} only a minor decrease in the fluorescence intensity of gallic acid was observed. The lack of efficient fluorescence quenching was also observed for the other model compounds investigated, which is in contrast to the observed quenching of the HS fluorescence upon Tb^{3+} addition. In Figure 6 the effect of Tb^{3+} on the fluorescence intensity of salicylic acid (as a further example of a model compound investigated) and of HS of different origins are compared. Shown are the normalized fluorescence intensity ratios I/I_0. For salicylic acid the fluorescence was not

quenched, which is obvious from the independence of the ratios I/I_0 on the concentration of Tb^{3+} added to the solution, the data points are randomly distributed around a ratio of one (see Figure 6). On the other hand the fluorescence of HS was quenched upon addition of Tb^{3+} ions which can be seen on the decreasing ratio of I/I_0. The extent of fluorescence quenching was highly dependent on the HS sample. The fluorescence of HS isolated from soil was quenched more effectively than the fluorescence of HS isolated from aquatic origin.

In the fluorescence quenching experiments a second luminescence signal originating from Tb^{3+} was observed (s. Figure 5).[39-41] While in the experiments the fluorescence of the model compounds and of HS stayed unchanged or was quenched, respectively, the Tb^{3+} luminescence increased in general with increasing concentration of Tb^{3+}. It is interesting to note that in control experiments in pure water in the absence of organic ligands under identical experimental conditions (Tb^{3+} concentration, excitation wavelength, slit widths, pH, ionic strength) no luminescence signal was observed for Tb^{3+}. Only at high Tb^{3+} concentrations (> 100 μM) a small luminescence signal from Tb^{3+} was detected. Moreover, the luminescence sensitisation of Tb^{3+} in complexes with model compounds was also investigate at pH 2, here no Tb^{3+} luminescence was observed, which indicates that only luminescence of complexed Tb^{3+} is detected.

In the presence of model compounds as well as HS even at very low Tb^{3+} concentrations (< μM) a Tb^{3+} sensitized luminescence signal was detected at pH values of 4, 5, and 6. Because of the formation of Tb^{3+} hydroxides no higher pH values were tested. The Tb^{3+} luminescence could be easily identified in the experimental emission spectra because of its characteristic, sharp luminescence peaks at λ_{em} = 489 nm and 544 nm (see Figure 5).

The observed increase of the Tb^{3+} luminescence intensity was dependent on the type of model ligand and on the HS origin. HS samples of aquatic origin showed a strong Tb^{3+} luminescence enhancement, while for soil derived HS the luminescence enhancement was considerably smaller. In order to compare the observed increase for different model compounds and for HS the luminescence intensity at λ_{em} = 544 nm was normalized. For the model compounds as well as for HS curves with different slopes at low Tb^{3+} concentrations were obtained. At higher Tb^{3+} concentrations well pronounced limiting plateaus were found for HS. In case of the model compounds this effect was less obvious and for gallic acid and 3,5-dihydroxy benzoic acid an almost linear relationship was shown in the data (see Figure 7 and 8).

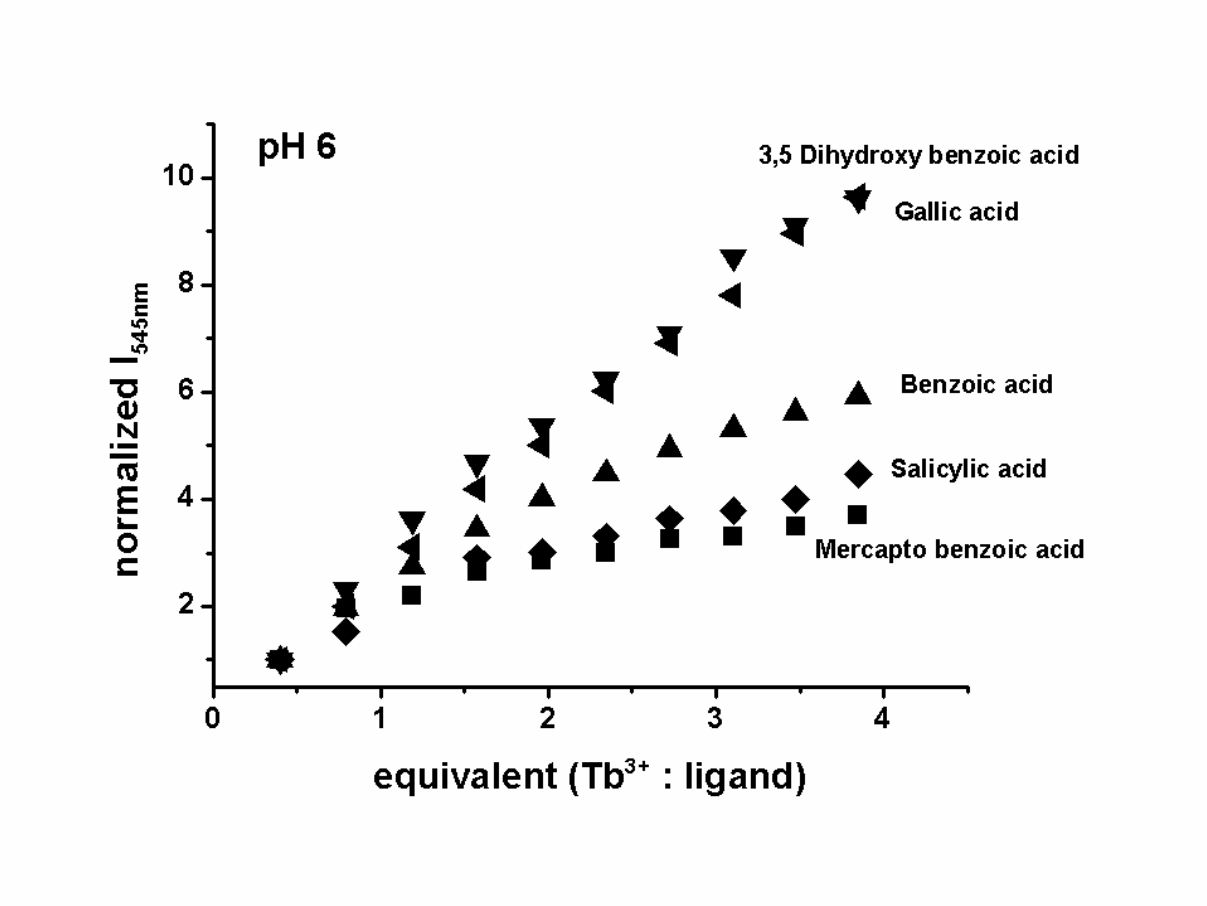

Figure 7 Luminescence enhancement of Tb^{3+} (λ_{em} = 544 nm) upon addition of model compounds at pH 4. Depending on the model compound investigated the excitation

wavelength was chosen 275 nm < l_{ex} < 325 nm. In order to compare the relative luminescence enhancement the signals were normalized to Tb^{3+} luminescence signal of the lowest concentration ($c_{Tb} = 4*10^{-5}$ M).

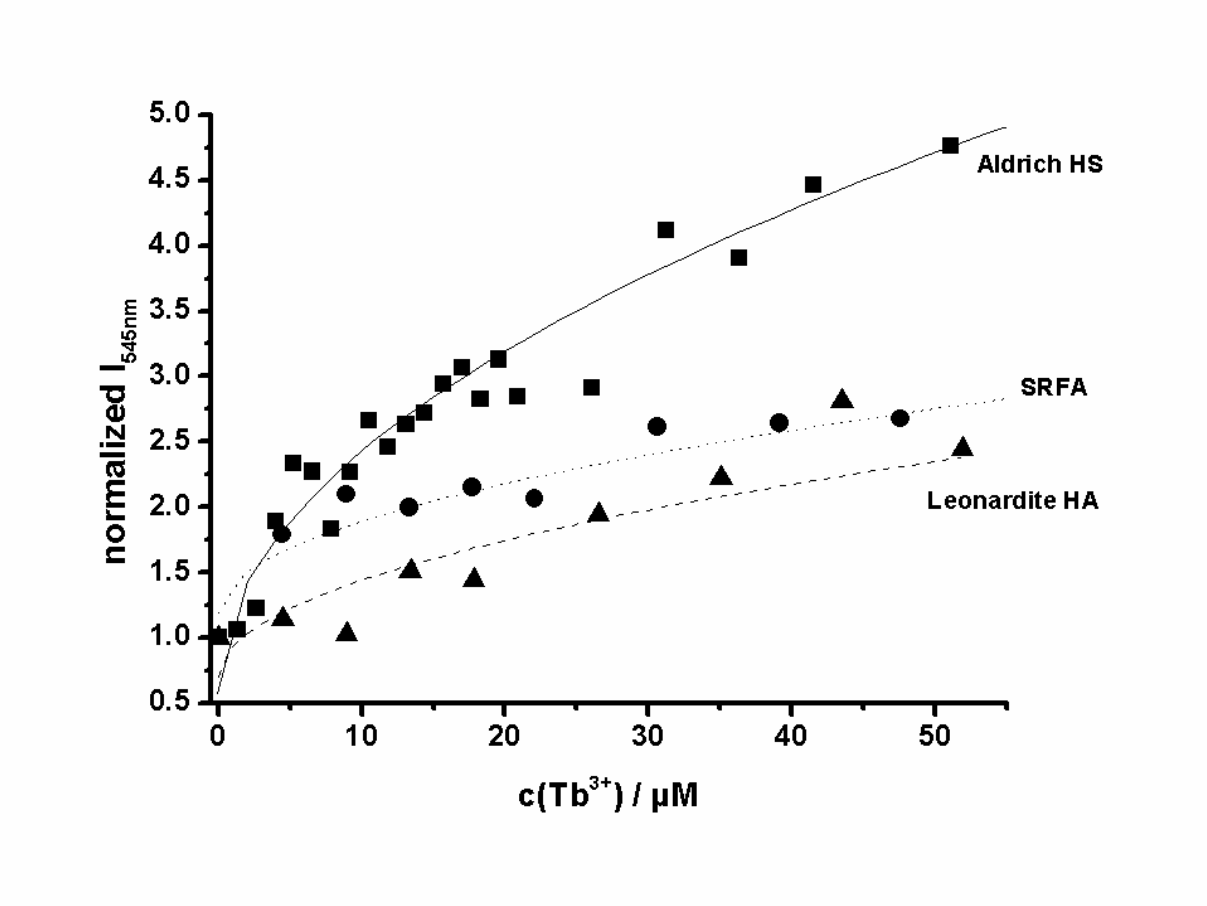

Figure 8 Luminescence enhancement of Tb^{3+} in the presence of HS (10 mg/L, pH 5) at λ_{em} = 544 nm normalized to the lowest Tb^{3+} concentration.

Further the luminescence decay of Tb^{3+} was investigated in the presence of model compounds and of HS. For Tb^{3+} a luminescence decay time of τ_{Tb} = 400 µs was measured which agreed well with the values reported in literature.[42-45] The fluorescence decay times of Tb^{3+} in the presence of model compounds were also mono-exponential and dependent on the molar ratio of model compound : Tb^{3+}, which is a consequence of the increased binding of Tb^{3+} with increasing ratio. It is interesting to note that the luminescence decay times of Tb^{3+} complexed with model compounds were shorter compared to Tb^{3+} (aq). For the samples

containing Tb^{3+} and HS, the observed experimental decays were no longer mono-exponential (s. Figure 10, left). Here, a complex luminescence decay was observed for Tb^{3+} bound to HS, which has to be attributed to the complexity of the HS sample and to the combination of energy transfer and backtransfer processes in the HS-Tb^{3+} complexes.

3.3 Inter-lanthanide energy transfer in lanthanide-HS complexes

Because of the unknown structure of HS the analysis of data from metal complexation experiments is difficult, mainly due to the fact that the stoichiometry of the formed complexes is unknown. This allows one only to calculate conditional binding constants (e.g., assuming a 1:1 stoichiometry). In order to circumvent this problem and to gain more insight into structural characteristics of HS that influence the metal binding, energy transfer between Tb^{3+} and Nd^{3+} both bound to HS was investigated. It is well established that the luminescence of Tb^{3+} is quenched by Nd^{3+}. The luminescence quenching is based on a dipole-dipole interaction and can be understood as a resonance energy transfer process between an excited donor (Tb^{3+}) and an acceptor (Nd^{3+}). Horrocks and co-workers used the inter-lanthanide energy transfer for the investigation of Ca^{2+}-binding sites in a number of enzymes.[46-50] The theory is well established and is based on a concept that was originally developed by Förster.[20-22] The basic idea is that the rate of energy transfer k_{ET} (and subsequently also the energy transfer efficiency E, where I_{DA} and I_D are the fluorescence intensities or luminescence lifetimes of the donor in the presence and absence of the acceptor, respectively) depends on $1/R^6$ where R is the distance between donor and acceptor.

$$k_{ET} = \frac{\Gamma \cdot \kappa^2 \cdot \Phi_D}{R_{DA}^6} J$$

$$E = 1 - \frac{I_{DA}}{I_D} \text{ and } E = 1 - \frac{\tau_{DA}}{\tau_D}$$

$$R = R_0\left(\frac{1}{E} - 1\right)^{\frac{1}{6}}$$

R_0 is the so-called Förster radius and is characteristic for the donor acceptor pair. The value of R_0 is defined by spectral overlap integral J, which contains the fluorescence spectrum ($I_F(\nu)$) of the donor and the absorption spectrum ($\varepsilon(\nu)$) of the acceptor, and the relative orientation of the transition dipole moments between donor und acceptor (described by the orientation factor κ). Due to the energy transfer the luminescence intensity and the luminescence lifetime of the donor (Tb^{3+}) are quenched. From measurements of the donor luminescence intensity (and/or the donor luminescence lifetime) in the absence and presence of acceptor (Nd^{3+}) the distance R between both can be calculated in case R_0 is known, like for Tb^{3+}/Nd^{3+}. Here, a R_0 of 9 Å is reported.[46-48]

In the experiments a titration of HS samples containing 10 µM Tb^{3+} with Nd^{3+} was performed and the luminescence intensity of Tb^{3+} at 544 nm was monitored. The concentration of Nd^{3+} was stepwise increased up to 100 µM. Under the experimental conditions applied no luminescence of directly excited Tb^{3+} was observed and only Tb^{3+} bound to HS was detected (s. paragraph 3.2). It was found that with increasing Nd^{3+} concentration the luminescence intensity of Tb^{3+} decreased indicating either an energy transfer from Tb^{3+} to Nd^{3+} both bound to HS or a replacement of HS-bound Tb^{3+} ions by Nd^{3+} ions.

Control experiments were performed to distinguish between those two processes. In order to check the contribution of Tb^{3+}-release from HS due to replacement with other lanthanide ions, La^{3+} was added. The chemical properties in terms of complexation

capabilities for the lanthanide ions should be very similar and La^{3+} and Nd^{3+} should have the same replacement capabilities for HS-bound Tb^{3+}. However, the spectroscopic properties of La^{3+} are very different from Nd^{3+}. La^{3+} has no energy acceptor capabilities and therefore, an energy transfer from Tb^{3+} to La^{3+} is not possible.[46-51] It was found that the contribution due to release of Tb^{3+} from the HS is small in the μM-concentration range. Thus, the observed decrease in luminescence intensity of Tb^{3+} upon addition of Nd^{3+} can be attributed mainly to an energy transfer between both ions when bound to HS.

In addition, the luminescence lifetime of Tb^{3+} in the presence and absence of Nd^{3+} was determined (see Figure 9). The lifetime of Tb^{3+} decreased with increasing Nd^{3+} concentration. No such decrease was observed for Tb^{3+}/Nd^{3+} solutions in water in the absence of HS. Here, the luminescence decay time of Tb^{3+} stayed unchanged in the presence of Nd^{3+} (see Figure 9).

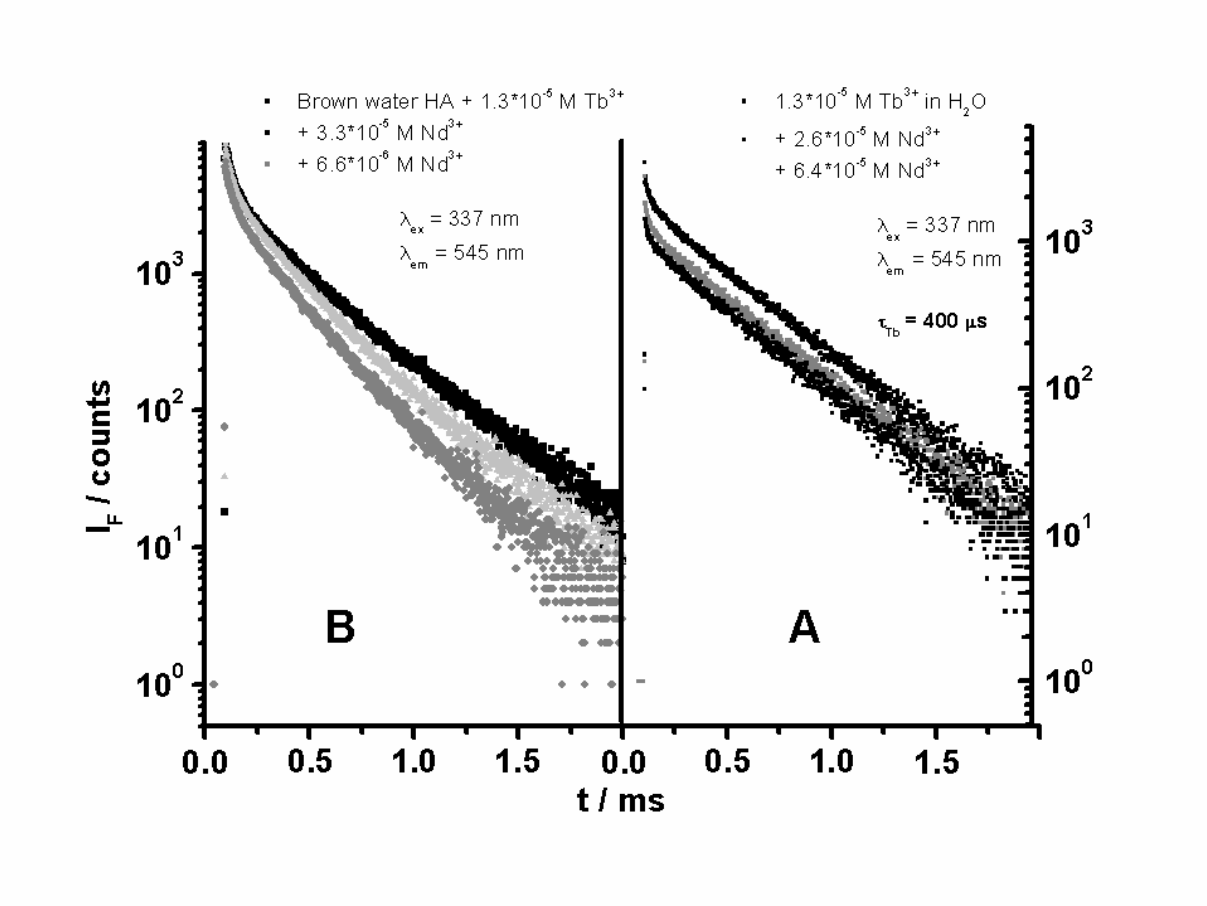

Figure 9 Dependence of Tb^{3+} luminescence decay on the presence of Nd^{3+} in a) pure water and b) bound to brown water HA (HO13 HA, 10 mg/L, pH 5)

The average distance *R* between Tb^{3+} and Nd^{3+} was determined for HS of different origin as well as for SRFA at different pH.

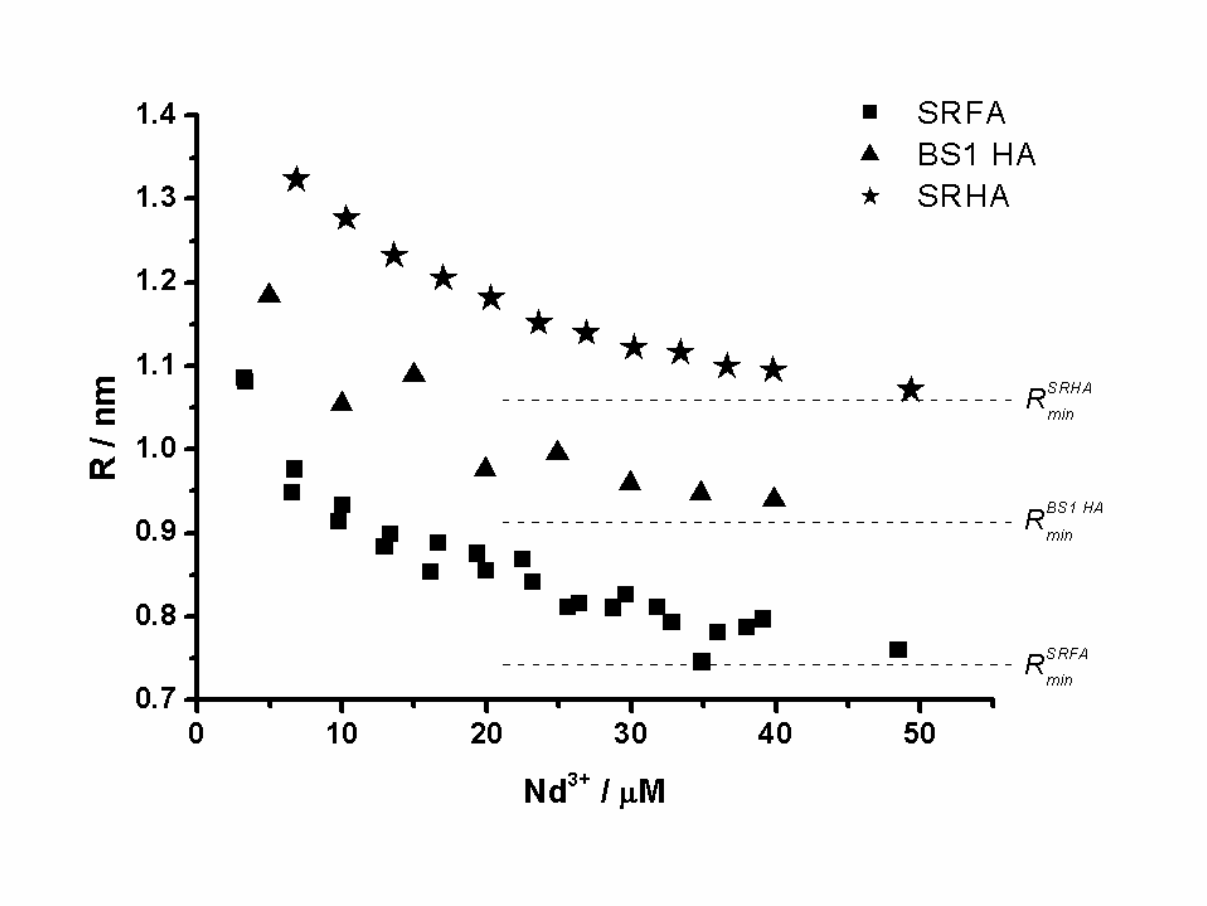

Figure 10 Dependence of the average distance *R* between Tb^{3+} (c_{Tb} = 10 μM) and Nd^{3+} bound to HS of different origin (pH 5, c_{HS} = 10 mg/L) on the concentration of Nd^{3+}.

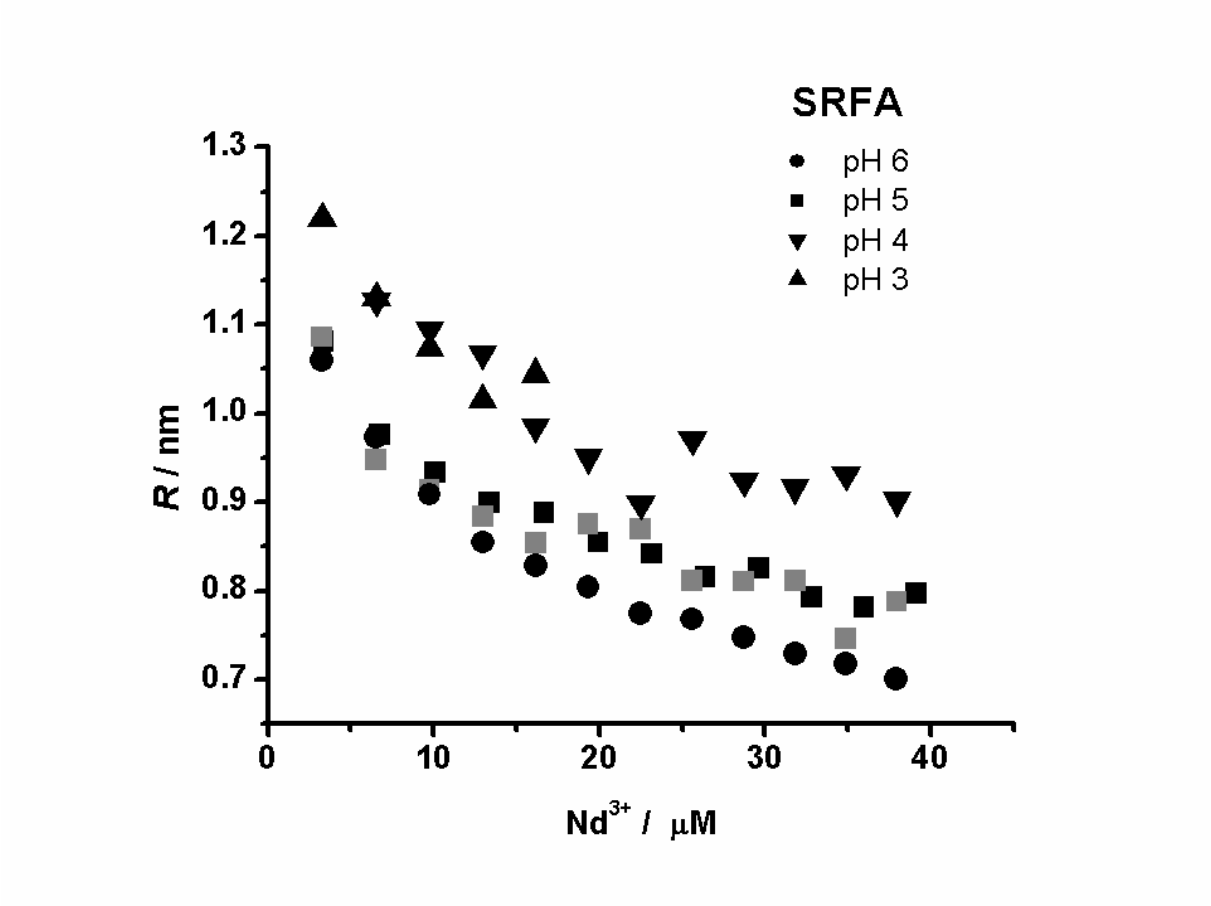

Figure 11 Dependence of the average distance *R* between Tb^{3+} (c_{Tb} = 10 µM) and Nd^{3+} bound to SRFA (pH 5, c_{HS} = 10 mg/L) on the concentration of Nd^{3+}. Compared is the influence of the pH on *R*.

In Figure 10 the dependence of *R* on the loading with Nd^{3+} for HS of different origin is shown for pH 5. With increasing Nd^{3+} concentration the average distance *R* between Tb^{3+}/Nd^{3+} bound to HS decreased. Depending on the Nd^{3+} concentration and on the origin of the HS, *R* values between 1.2 nm and 0.85 nm were calculated. It is interesting to note that for each HS the average distance *R* approached a minimum distance R_{min} which seems to be specific for the HS investigated.

In Figure 11 the dependence of *R* on the loading with Nd^{3+} of SRFA at different pH is compared. At each pH the average distance between Tb^{3+} and Nd^{3+} approached a limiting distance R_{min}. The distance *R* was clearly dependent on the pH. The average distance *R* was larger at lower pH, e.g., for a Nd^{3+} concentration of 20 μM we found at pH 4 an average distance of 0.95 nm while at pH 6 an average distance *R* of 0.8 nm was calculated.

4. DISCUSSION

The fluorescence emission spectra of HS are broad, without a vibronic structure and are located in the spectral range 350 nm < λ_{em} < 600 nm with a maximum around 470 nm ± 15 nm.[24-27,29,34,35] The fluorescence efficiency and the location of the fluorescence maximum are dependent on solution parameters of which the pH is the most important.[26,31,33,36,37] In addition, the fluorescence decay kinetic of HS is highly complex.[52-55] As possible reasons for the observed complexity have been discussed 1) the vast heterogeneity of the HS themselves, 2) various intra- and intermolecular interaction processes like energy transfer between different chromophores of HS, and 3) processes that involve excited state reactions like proton transfer (excited state intramolecular proton transfer, ESIPT) or conformational motions (e.g., twisted intramolecular charge transfer, TICT). The steady-state and time-resolved fluorescence properties of the model compounds investigated resemble many of the HS fluorescence characteristics. Especially, for the medium pH range (3 < pH < 9) the complexity of the HS fluorescence decay as well as the shift of the fluorescence maximum in the TRES are also found in the observed fluorescence of the model compounds. For the model compounds the observed complexity of the fluorescence can be attributed to excited state reactions that involve the transfer of protons (e.g., ESIPT and interaction with water) and can be characterized by the so-called Förster cycle.[20,21] The importance of proton transfer

reactions in the excited state is further supported by the observation that upon addition of Tb^{3+} the temporal and spectral fluorescence characteristics are changed. This was previously reported for HS and Eu^{3+} and the possible contribution of ESIPT reactions has been suggested.[55] The observed alterations in the temporal and spectral fluorescence characteristics of model compounds add further evidence to it.

While the temporal and spectral characteristics of the model compounds were in good agreement with the HS fluorescence, a major difference was observed in the fluorescence quenching studies with Tb^{3+}. The intrinsic fluorescence of HS was quenched upon Tb^{3+} addition, while for the majority of the model compounds no (or only very minor) fluorescence quenching was found. The latter is not unexpected since for f-elements only a small spin-orbit coupling should be operative in complexes because the f-electrons are shielded by the closed s- and p-shells (in case of Tb^{3+} the 4f-electrons are shielded by 5s- and 5p-orbitals). It is more likely that other processes cause the HS fluorescence quenching upon addition of Tb^{3+} (and in general by lanthanide ions): 1) the competition between H^{+} and Tb^{3+} for carboxyl- and hydroxyl-groups and subsequently the alteration of photo-induced processes connected to these groups like ESIPT and 2) the influence on the molecular flexibility caused by intra- or intermolecular bridging (e.g., comparable to the formation of H-bonds) which limits the rotational freedom of parts of the molecule. This could subsequently change the fluorescence of the molecule in case photo-induced geometry changes are involved in the fluorescence process of HS. Twisted intramolecular charge transfer (TICT) processes are an example for such intramolecular rotations.

The fact that the fluorescence of the model compounds is not quenched by Tb^{3+} makes it attractive to assume that intramolecular (and possibly also intermolecular if association is

considered as well) reorientations play a major part in the fluorescence process of HS.[54,55] Metal ions bound to HS can interfere with these processes by the formation of complexes with HS and hence limiting the rotational freedom of molecular moieties. The observed netto-effect would than be a fluorescence quenching because the fluorescing form of the HS can no longer be formed within the photoinduced process.

The observed sensitization of the Tb^{3+} luminescence by organic ligands has been observed earlier and was attributed to an energy transfer process from the organic ligand to the Tb^{3+} ion.[56-59] The triplet state of the organic ligand has been identified as the energy-transferring state, which also explains that no fluorescence quenching was observed in the case of model ligands and supports the assumption that in case of HS the limitation of conformational motions is a major reason for the observed fluorescence quenching by Tb^{3+}. The energies of the triplet state of the organic ligand and the emitting $^5D_4$-state of Tb^{3+} determine the efficiency of energy transfer and the possible radiationless decay due to an energy back transfer process from Tb^{3+} to the ligand.[59] The observed luminescence quantum efficiency of the complex is in many cases smaller than the luminescence quantum efficiency of the Tb^{3+}(aq) ion itself due to an effective energy back transfer. However, because of the very low molar extinction coefficients of Tb^{3+} (< 1 $M^{-1}cm^{-1}$) the so-called "antenna effect" leads to an increase of the observable luminescence intensity of the organic complex (under identical excitation and emission conditions).[58,59] This is related to the much larger extinction coefficients of the ligands (> 1000 $M^{-1}cm^{-1}$).

For the model compounds the normalized intensity of the sensitized Tb^{3+} luminescence yielded curves with different slopes and in some case almost a linear relationship. Comparable well-pronounced plateaus like for HS were not found in the investigated

concentration range. For HS the height of the plateaus formed was dependent on the origin of the HS. A direct comparison between model compounds and HS is difficult since the number of binding sites and the calculation of a molar ratio between HS and Tb^{3+} is not possible like it is the case of the model compounds. The fact that the observed luminescence sensitization of Tb^{3+} upon binding to HS depends on the origin of the HS reflects the difference in structure in terms of the presence of chromophores with 1) suitable triplet energies and 2) of $RCOO^-$- and RO^-- groups connected to those chromophores. For the soil derived HS samples the observed luminescence sensitization was considerably smaller in comparison to the HS of aquatic origin. This indicates that in those samples the triplet energy might be to close to the $^5D_4$ energy of Tb^{3+} allowing an effective energy back transfer from Tb^{3+} to the HS triplet state.

The measurement is very sensitive and specific because of 1) the sharp, well-defined Tb^{3+} luminescence peaks, and 2) only sensitized luminescence is observed, hence only the luminescence of the bound Tb^{3+} contributes to the detected luminescence signal. The measurement of fluorescence enhancement is easier and more sensitive compared to luminescence quenching techniques since the detection of photons against a low background is superior to the detection of a (minor) decrease of a luminescence signal. In the experiments the Tb^{3+} luminescence is well separated from the HS fluorescence and can be easily detected, especially with a time-gated detection scheme since the Tb^{3+} luminescence is observed on a μs timescale while the HS fluorescence decay on a ns-timescale. The limitation of the detection of sensitized luminescence is the still unknown connection between metal binding sites and HS chromophores, that have suitable triplet state energies. The exact mechanism of the energy transfer between HS and Tb^{3+} is not known yet and subject of ongoing research. Two basic mechanism with different dependencies of the distance between donor and

acceptor have to be distinguished: 1) the dipole-dipole mechanism with its $1/R^6$-relationship and 2) the exchange mechanism, in which the rate of the energy transfer step decreases exponentially with the distance between donor and acceptor. A first rough calculation of a hypothetical R_0 between HS and Tb^{3+} based on the fluorescence spectrum of Suwannee River fulvic acid and the absorption spectrum of Tb^{3+} yielded a value of approximately 4 Å, which is quite small and suggests that under the assumption made the exchange mechanism is the more probable. That would mean that specifically the fraction of chromophores with metal binding capabilities in close neighbourhood and with suitable triplet energies could be probed. Here, further research is needed to shed more light on the connection between metal binding sites and chromophores.

The limitations arising from the unknown HS structure can be circumvented with the introduction of Nd^{3+} and the use of the inter-lanthanide energy transfer as a molecular ruler. The spectroscopy properties of the Tb^{3+}/Nd^{3+} donor-acceptor pair are well characterized in terms of the operative energy transfer mechanism (dipole-dipole mechanism) and subsequently of the Förster distance R_0, which is 9.3 Å.[46-50] Here, only the relative distance of the bound Tb^{3+} and bound Nd^{3+} determines the energy transfer efficiency. Unbound Tb^{3+} or unbound Nd^{3+} ions do not interfere with the measurement as it was shown in control experiments. Although information on the absolute structure of HS is still not accessible, relative information on HS conformation and how the conformation of HS is altered by solution parameters (e.g., pH, ionic strength, addition of metal ions) can be monitored – in solution and under environmental relevant concentrations of a few mg/L. The R_{min} seems to be specific for the type of HS and reflects structural (binding) properties of HS as it was shown for HS of different origin.

5. CONCLUSIONS

Excited state reactions seem to play an important role in the overall fluorescence process of HS, especially proton transfer reactions and conformational reorientations after excitation are the major processes involved. Both processes are strongly influenced upon metal ion complexation because of the competition for binding sites between metal ions and protons and because of an inter- and intramolecular "bridging effect" of metal ions that limits the rotational freedom of the HS molecules. Experiments with other model compounds and biopolymers (e.g., lignin and chitin) are planned and will help to further improve our understanding of those processes in HS. Moreover, the results underline limitations of the HS fluorescence quenching approach for the determination of conditional binding constants with metals. The contributions of real fluorescence quenching and spectral shifts in the fluorescence spectrum need to be elucidated, which is very difficult with standard 2D-fluorescence spectra. A solution might be the measurement of excitation-emission matrices in order to get the complete picture of the alterations in the HS fluorescence upon metal complexation. With the application of Tb^{3+} (and also Eu^{3+}) as luminescence probe, the metal complexation can be monitored from a different angle. Only bound Tb^{3+} is detected after indirect excitation via an intramolecular energy transfer step. The combination of HS fluorescence quenching and luminescence enhancement via energy transfer could be helpful for the determination of better defined stability constants from fluorescence experiments with HS. For the energy transfer the energy of the triplet state of the chromophore is the most important parameter, which limits the luminescence enhancement of Tb^{3+} to a certain group of chromophores. The relative abundance of chromophores with suitable triplet state can be an interesting parameter for the structural characterization of HS.

The limitations of the unknown structure of HS can be overcome with the application of interlanthanide energy transfer measurements. Here, only the distance between Tb^{3+} and Nd^{3+} are important when bound to HS. The measurements are very sensitive and can be performed at the μM-concentration level. Because of the great sensitivity samples in realistic concentration ranges can be investigated. Effects of pH, ionic strength or the addition of metal ions (not necessarily lanthanides) on the conformation of HS can be monitored. Currently we are exploiting the interlanthanide energy transfer approach for the investigation of inter- and intramolecular association reactions of HS.

ACKNOWLEDGEMENTS

The authors wish to thank Melanie Hans and Sascha Prenzel for their help with the preparation of samples. They also greatly appreciate the support of Prof. H.-G. Löhmannsröben and are thankful for using the instrumental equipment. Further, the authors thank Prof. F.H. Frimmel for the supply of the humic substances HO13 HA and BS1 HA.

6. REFERENCES

1. Dobbs JC, Susetyo W, Carreira LA, Azarraga LV. Competitive binding of protons and metal ions in humic substances by lanthanide ion probe spectroscopy. *Analytical Chemistry*, 1989, 61: 1519-1524.
2. Ryan DK, Weber JH. Fluorescence quenching titration for determination of complexing capacities and stability constants of fulvic acid. *Analytical Chemistry*, 1982, 54: 986-990.

3. Saar RA, Weber JH. Comparison of spectrofluorometry and ion-selective electrodes potentiometry for determination of complexes between fulvic acid and heavy-metal ions. *Analytical Chemistry*, 1980, 52: 2095-2100.
4. Gamble DS, Underdown AW, Langford CH. Copper(II) titration of fulvic acid ligand sites with theoretical, potentiometric, and spectrophotometric analysis. *Analytical Chemistry*, 1980, 52: 1901-1908.
5. Wu SL, Horrocks WdeW. General Method for the determination of Stability constants of lanthanide ion chelates by ligand-ligand competition: laser-excited Eu^{3+} luminescence excitation spectroscopy. *Analytical Chemistry*, 1996, 68: 394-401.
6. Smith DS, Kramer JR. Fluorescence analysis for multi-site aluminium binding to natural organic matter. *Environment International*, 1999, 25: 295-306.
7. Smith DS, Kramer JR. Multi-site aluminium speciation with natural organic matter using multiresponse fluorescence data. *Analytica Chimica Acta*, 1998, 363: 21-29.
8. Bidoglio G, Ferrari D, Selli E, Sena F, Tamborini G. Humic acid binding of trivalent Tl and Cr studied by synchronous and time-resolved fluorescence. *Environmental Science and Technology*, 1997, 31: 3536-3543.
9. Da Silva JCGE, Ferreira MA, Machado AASC, Rey F. Classification of binding sites of Al(III) in fulvic acid extracted from leaf litters and soils by synchronous fluorescence spectroscopy and multidimensional chemometric analysis. *Analytica Chemica Acta,* 1996, 333: 71-82.
10. Thomason JW, Susetyo W, Carreira LA. Fluorescence studies of metal-humic complexes with the use of lanthanide ion probe spectroscopy. *Applied Spectroscopy*, 1996, 50: 401-408.

11. Machado AASC, Da Silva JCGE, Maia JAC. Multi-wavelength analysis of synchronous fluorescence spectra of the complexes between a soil fulvic acid and Cu(II). *Analytica Chimica Acta*, 1994, 292: 121-132.
12. Cabaniss SE. Synchronous fluorescence spectra of metal-fulvic acid complexes. *Environmental Science and Technology*, 1992, 26: 1133-1139.
13. Shuman, MS. Dissociation pathways and species distribution of aluminium bound to an aquatic fulvic acid. *Environmental Science and Technology*, 1992, 26: 593-598.
14. Seritti A, Morelli E, Nannicini L, Giambelluca A, Scarano G. Fluorescence emission characteristics of naturally occuring organic matter in relation to metal complexation studies. *The Science of the Total Environment*, 1994, 148: 79-81.
15. Susetyo W, Carreira LA, Azarraga LV, Grimm DM. Fluorescence techniques for metal-humic interactions. *Fresenius Journal of Analytical Chemistry*, 1991, 339: 624-635.
16. Cabaniss SE, Shuman MS. Fluorescence quenching measurements of copper-fulvic acid binding. *Analytical Chemistry*, 1988, 60: 2418-2421.
17. Ryan DK, Ventry LS, Cabaniss SE, Shuman MS. Exchange of comments on fluorescence quenching measurements of copper-fulvic acid binding. *Analytical Chemistry*, 1990, 62: 1523-1526.
18. Stenson AC, Marshall AG, Cooper WT. Exact masses and chemical formulas of individual Suwannee river fulvic acids from ultrahigh resolution electrospray ionization fourier transform ion cyclotron resonance mass spectra. *Analytical Chemistry*, 2003, 75: 1275-1284.
19. Kumke MU, Specht CH, Brinkmann T, Frimmel FH. Alkaline hydrolysis of humic substances – Spectroscopic and chromatographic investigations. *Chemosphere,* 2001, 45: 1023-1031.

20. Förster T. *Fluoreszenz organischer Verbindungen*. Göttingen: Vandenhoeck&Ruprecht, 1951.
21. Valeur B. *Molecular Fluorescence*. Weinheim: Wiley-VCH, 2002.
22. Clegg RM. Fluorescence resonance energy transfer. In: Winefordner JD, Wang XF, Herman B eds. *Chemical Analysis: Fluorescence imaging spectroscopy and microscopy*. New York: John Wiley & Sons, Volume 137, 1996: 179-254.
23. Abbt-Braun G, Frimmel FH. The relevance of reference materials – isolation and general characterization. In: Frimmel FH, Abbt-Braun G, Heumann KG, Hock B, Lüdemann HD, Spiteller M eds. *Refactory organic substances in the environment*. Weinheim: Wiley-VCH, 2002: 1-54.
24. Kumke MU, Frimmel FH. Stationary and time-resolved fluorescence for humic substances characterization. In: Frimmel FH, Abbt-Braun G, Heumann KG, Hock B, Lüdemann HD, Spiteller M eds. *Refactory organic substances in the environment*. Weinheim: Wiley-VCH, 2002: 215-231.
25. Illenseer C, Löhmannsröben HG, Skrivanek T, Zimmermann U. Laser spectrosopy of humic substances. In: Ghabbour EA, Davies G eds. *Understanding humic substances – Advanced methods, properties and applications*. Cambridge: RSC, 1999: 129-145.
26. Provenzano MR, Miano TM, Senesi N. Concentration and pH effects on the fluorescence spectra of humic acid-like soil fungal polymers. *The Science of the Total Environment*, 1989, 81/82: 129-136.
27. Senesi N, Miano TM, Provenzano MR, Brunetti G. Spectroscopic and compositional comparative characterization of I.H.S.S. reference and standard fulvic and humic acids of various origin. *The Science of the Total Environment*, 1989, 81/82: 143-156.
28. Schmiedel U, Frimmel FH. Fluorescence of chlorinated fulvic acids. *Vom Wasser*, 1991, 77: 333-348.

29. Senesi N, Miano TM, Provenzano MR. Fluorescence spectroscopy as a means of distinguishing fulvic and humic acids from dissolved and sedimentrary aquatic sources and terrestrial sources. In: Bhattacharji S, Friedman GM, Neugebauer HJ, Seilacher A. Allard B, Boren H, Grimwall A eds. *Lecture notes in earth sciences: Humic substances in the aquatic and terrestrial environment*. Berlin: Springer-Verlag, Volume 33, 1991: 63-73.
30. Patterson HH, Cronan CS, Lakshman S, Plankey BJ, Taylor TA. Comparison of soil fulvic acids using synchronous scan fluorescence spectroscopy, FTIR, titration and metal complexation kinetics. *The Science of the Total Environment*, 1992, 113: 179-196.
31. Pullin MJ, Cabaniss SE. Rank analysis of the pH-dependent synchronous fluorescence spectra of six standard humic substances. *Environmental Science and Technology*, 1995, 29: 1460-1467.
32. Ahmad SR, Reynolds DM. Synchronous fluorescence spectroscopy of wastewater and some potential constituents. *Water Research*, 1995, 29: 1599-1602.
33. Casassas E, Marques I, Rauler R. Study of acid-base properties of fulvic acids using fluorescence spectrometry and multivariate curve resolution methods. *Analytica Chimica Acta*, 1995, 310: 473-484.
34. Mobed JJ, Hemmingsen SL, Autry JL, McGown LB. Fluorescence characterization of IHSS humic substances: total luminescence spectra with absorbance correction. *Environmental Science and Technology*, 1996, 30: 3061-3065.
35. Matthews BJH, Jones AC, Theodorou NK, Tudhope AW. Excitation-emission-matrix fluorescence spectroscopy applied to humic acid bands in coral reefs. *Marine Chemistry*, 1996, 55: 317-332.

36. Da Silva JCGE, Machado AASC, Silva CSPCO. Simultaneous use of evolving factor analysis of fluorescence spectral data and analysis of pH titration data for comparison of the acid-base properties of fulvic acids. *Analytica Chimica Acta*, 1996, 318: 365-372.
37. Da Silva JCGE, Machado AASC. Procedure for the classification of fulvic acids and similar substances based on the variation with pH of their synchronous fluorescence spectra. *The Analyst*, 1997, 122: 1299-1305.
38. Kalbitz K, Geyer S, Geyer W. A comparative characterization of dissolved organic matter by means of original aqueous samples and isolated humic substances. *Chemosphere*, 2000, 40: 1305-1312.
39. Panak P, Klenze R, Kim JI, Wimmer H. A study of intramolecular energy transfer in Cm(III) complexes with aromatic ligands by time-resolved laser fluorescence spectroscopy. *Journal of Alloys and Compounds*, 1995, 225: 261-266.
40. Kim JI, Rhee DS, Wimmer H, Buckau G, Klenze R. Complexation of trivalent actinide ions (Am^{3+}, Cm^{3+}) with humic acid: a comparison of different experimental methods. *Radiochimica Acta*, 1993, 62: 35-43.
41. Wimmer H, Kim JI, Klenze R. A direct speciation of Cm(III) in natural aquatic systems by time-resolved laser-induced fluorescence spectroscopy (TRLFS). *Radiochimica Acta*, 1992, 58/59: 165-171.
42. Horrocks WDeW, Albin M. Lanthanide ion luminescence in coordination chemistry and biochemistry. In: Lippard SJ ed. *Progress in inorganic chemistry*. New York: John Wiley & Sons, Volume 31, 1984: 1-104.
43. Horrocks WdeW, Sudnick DR. Lanthanide ion luminescence probes of the structure of biological macromolecules. *Accounts of Chemical Research*, 1981, 14: 384-392.

44. Sabbatini N, Guardigli M, Lehn, JM. Luminescent lanthanide complexes as photochemical supramolecular devices. *Coordination Chemistry Reviews*, 1993, 123: 201-223.

45. Selvin PR. Principles and biophysical applications of lanthanide-based probes. *Annual Reviews in Biophysical and Biomolecular Structure*, 2002, 31: 275-302.

46. Horrocks WdeW, Rhee MJ, Snyder AP, Sudnick DR. Laser-induced metal ion luminescence: interlanthanide ion energy transfer distance measurements in the calcium-binding proteins, Parvalbumin and Thermolysin. Metalloprotein models address a photophysical problem. *Journal of the American Chemical Society*, 1980, 102: 3650-3652.

47. Snyder AP, Sudnick DR, Arkle VK, Horrocks WdeW. Lanthanide ion luminescence probes. Characterization of metal ion binding sites and intermetal energy transfer distance measurements in calcium-binding proteins. 2. Thermolysin. *Biochemistry*, 1981, 20: 3334-3339.

48. Horrocks WDeW, Collier WE. Lanthanide ion luminescence probes. Measurement of distance between intrinsic protein fluorophores and bound metal ions: Quantification of energy transfer between Tryptophan and terbium(III) or europium(III) in the calcium-binding protein parvalbumin. *Journal of the American Chemical Society,* 1981, 103: 2856-2862.

49. Breen PJ, Hild EK, Horrocks WDeW. Spectroscopic studies of metal ion binding to Tryptophan-containing parvalbumin. *Biochemistry*, 1985, 24: 4991-4997.

50. Mulqueen P, Tingey JM, Horrocks WDeW. Characterization of lanthanide(III) ion binding to calmodulin using luminescence spectroscopy. *Biochemistry*, 1985, 24: 6639-6645.

51. Lis S, Elbanowski M, Makowska B, Hnatejko Z. Energy transfer in solution of lanthanide complexes. *Journal of Photochemistry and Photobiology A: Chemistry*, 2002, 150: 233-247.

52. Kumke MU, Abbt-Braun G, Frimmel FH. Time-Resolved Fluorescence Measurements of Aquatic Natural Organic Matter. *Acta Hydrochimica Hydrobiologica*, 1998, 26: 73–81.

53. Kumke MU, Tiseanu C, Abbt-Braun G, Frimmel FH. Fluorescence Decay of Natural Organic Matter (NOM) – Influence of Fractionation, Oxidation, and Metal Ion Complexation. *Journal of Fluorescence*, 1998, 8: 309–318.

54. Frimmel FH, Kumke MU. Fluorescence decay of humic substances (HS) – A comparative study. In: Davies G, Ghabbour EA eds. *Humic Substances: structure, properties, and uses*. Cambridge: RSC, 1998: 113 – 122.

55. Tiseanu C, Kumke MU, Frimmel FH, Klenze R, Kim JI. Time-Resolved Spectroscopy of Fulvic Acid and Fulvic Acid Complexed with Eu^{3+} - A Comparative Study. *Journal of Photochemistry and Photobiology A*, 1998, 117: 175–184.

56. Buono-Core GE, Li H, Marciniak B. Quenching of excited states by lanthanide ions and chelates in solution. *Coordination Chemistry Reviews*, 1990, 99: 55-87.

57. Wu P, Brand L. Resonance energy transfer: methods and applications. *Analytical Biochemistry*, 1994, 218: 1-13.

58. Selvin PR. Lanthanide-based resonance energy transfer. *IEEE Journal of Selected Topics in Quantum Electronics*, 1996, 2: 1077-1087.

59. Alpha B, Ballardini R, Balzani V, Lehn JM, Perathoner S, Sabbatini N. Antenna effect in luminescent lanthanide cryptates: a photophysical study. *Photochemistry and Photobiology*, 1990, 52: 299-306.